

Growth of spatial correlations in the aging of a simple structural glass

Azita Parsaeian and Horacio E. Castillo

Department of Physics and Astronomy, Ohio University, Athens, OH, 45701, USA

(Dated: October 27, 2006)

The presence of dynamical heterogeneities is increasingly being recognized as a crucial factor in the understanding of the glass transition. Here we present a detailed numerical study of dynamical spatial correlations in the aging regime of a simple binary Lennard-Jones glass former. We find that for most waiting times t_w and final times t , both the dynamical susceptibility $\chi_4(t, t_w)$ and the dynamical correlation length $\xi_4(t, t_w)$ can be approximated as products of two factors: i) a waiting time dependent scale and ii) a scaling function dependent on t, t_w only through the value of the intermediate scattering function $C(t, t_w)$. In both cases, the t_w -dependent scales show power law growth with exponents consistent with the dynamical susceptibility being simply proportional to the dynamic correlation volume. However, the scaling functions dependent on $C(t, t_w)$ paint a slightly more complex picture, where both the strength of the correlations and the correlation volume play a role in determining the dynamical susceptibility.

PACS numbers: PACS: 64.70.Pf, 61.20.Lc, 61.43.Fs

When a liquid's temperature is rapidly reduced, it can become supercooled and eventually undergo a transition into a glass state. As the transition is approached, the relaxation time and the viscosity grow by several orders of magnitude. The glass transition is the point at which the relaxation time of the liquid becomes longer than a fixed laboratory timescale¹. Consequently, a system in the glass state is out of thermodynamic equilibrium. In particular, *physical aging* is observed: *time translation invariance (TTI)* is broken, i.e. correlations between observables at times t_w (the *waiting time*) and t (the *final time*) depend non-trivially on both times, and not just on their difference $t - t_w$ ².

Several observations about the glass transition, including the rapidly increasing relaxation timescales, the presence of non-exponential relaxation, and the violation of Stokes-Einstein relations between viscosity and diffusivity, have motivated the assumption that *dynamical heterogeneities* are present in the supercooled liquid^{3,4}. *Dynamical heterogeneities* are nanometer-scale regions containing molecules that rearrange cooperatively at very different rates compared to the bulk^{3,4}. After being postulated on the basis of bulk measurements, dynamical heterogeneities have been directly observed in local probe experiments, not only in supercooled liquids^{5,6} but also in glasses^{7,8,9,10}. However, except for the pioneering work by Parisi¹¹, most simulations studying dynamical heterogeneities in off-lattice models of structural glasses have focused on the supercooled regime^{12,13,14}.

In this Letter we present a simulation study of dynamic spatial correlations in the aging regime of a continuous-space, quasi-realistic glass model, with the goal of characterizing in detail their extent, space dependence, and time dependence. We discuss the spatial correlations of density fluctuations, which have been used before to characterize dynamical heterogeneities in the supercooled regime^{12,13,14}, and we also study the spatial dependence of the correlations of particle displacements, which provides a way of probing the geometrical structure of the

relaxation behavior in the aging regime. A theoretical framework that postulates the presence of local fluctuations in the age of the sample^{15,16,17,18}, predicts that probability distributions of local fluctuations in the aging regime are approximately independent of t_w at fixed values of the two-time global correlation $C_{\text{global}}(t, t_w)$. This prediction has been confirmed in simulations of both spin glasses^{16,17,18} and structural glasses¹⁹ (where C_{global} is the self part of the intermediate scattering function). Motivated by this scaling, we examine the possible presence of scaling behavior as a function of C_{global} and t_w in the dynamic spatial correlations.

In order to probe the spatial density correlations, we use the 4-point (2-time, 2-position) correlation function²⁰:

$$g_4(\mathbf{r}, t, t_w) = \frac{1}{N\rho} \left\langle \sum_{ik} \delta(\mathbf{r} - \mathbf{r}_k(t_w) + \mathbf{r}_i(t_w)) \right. \quad (1)$$

$$\left. \times w(|\mathbf{r}_i(t) - \mathbf{r}_i(t_w)|) w(|\mathbf{r}_k(t) - \mathbf{r}_k(t_w)|) \right\rangle - \left\langle \frac{Q(t, t_w)}{N} \right\rangle^2;$$

where $Q(t, t_w) \equiv \sum_{i=1}^N w(|\mathbf{r}_i(t_w) - \mathbf{r}_i(t)|)$ and $w(|\mathbf{r}_1 - \mathbf{r}_2|)$ is an overlap function which is unity for $|\mathbf{r}_1 - \mathbf{r}_2| \leq a$ and zero otherwise. ($a \equiv 0.3 \sigma_{AA}$ is an upper bound for the typical amplitude of the vibrational motion²⁰.) By integrating $g_4(\mathbf{r}, t, t_w)$ over space, the generalized 4-point density susceptibility $\chi_4 \equiv \int d^3\mathbf{r} g_4(\mathbf{r}, t, t_w)$ ²⁰ is obtained. The self part of the intermediate scattering function $C = C_{\text{global}}(t, t_w) = \frac{1}{N} \sum_{j=1}^N \exp(i\mathbf{q} \cdot (\mathbf{r}_j(t) - \mathbf{r}_j(t_w)))$, can be used as a measure of the correlation between the configurations of the system at times t_w and t : it is unity when $t = t_w$ and decays to zero when $t - t_w \gg t_w$ ^{2,21,22}.

We performed 4250 independent molecular dynamics runs (250 "longer" runs and 4000 "shorter" runs) for the binary Lennard-Jones (LJ) system of Ref.²¹, which has a mode coupling critical temperature $T_c = 0.435$. A system of 8000 particles was equilibrated at a temperature $T_0 = 5.0$, then instantly quenched to $T = 0.4$, and then allowed to evolve at that temperature for 10^5 (2.5×10^3) Lennard-

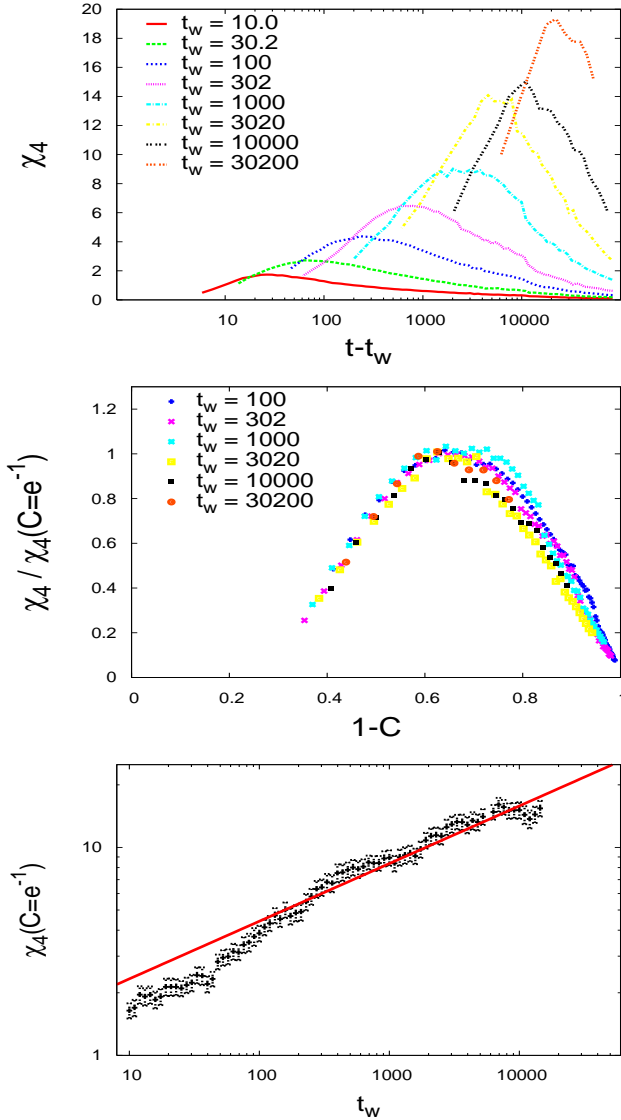


FIG. 1: (Color online) *Top panel*: Generalized density susceptibility χ_4 as a function of the time difference $t - t_w$, for waiting times $t_w = 10.0, \dots, 30200$. As the waiting time grows, both the position and strength of the maximum increase. *Middle panel*: Rescaled density susceptibility versus $1 - C$. *Bottom panel*: Rescaling factor of the density susceptibility, $\chi_4(C = 1/e)$, versus the waiting time. The straight line is a fit to $\chi_4(C = 1/e) = a t_w^b$, with fitting parameters $b = 0.277 \pm 0.008$ and $a = 1.232 \pm 0.008$.

Jones time units in the “longer” (“shorter”) runs. The origin of times was taken at the instant of the quench.

We first discuss the 4-point density susceptibility χ_4 . In the top panel of Fig. 1 we see that for fixed waiting time t_w , as the time difference $t - t_w$ increases, the spatial correlation increases till it reaches a maximum, and then decreases. The value of the correlation χ_4 at the peak and the time difference $t - t_w$ at

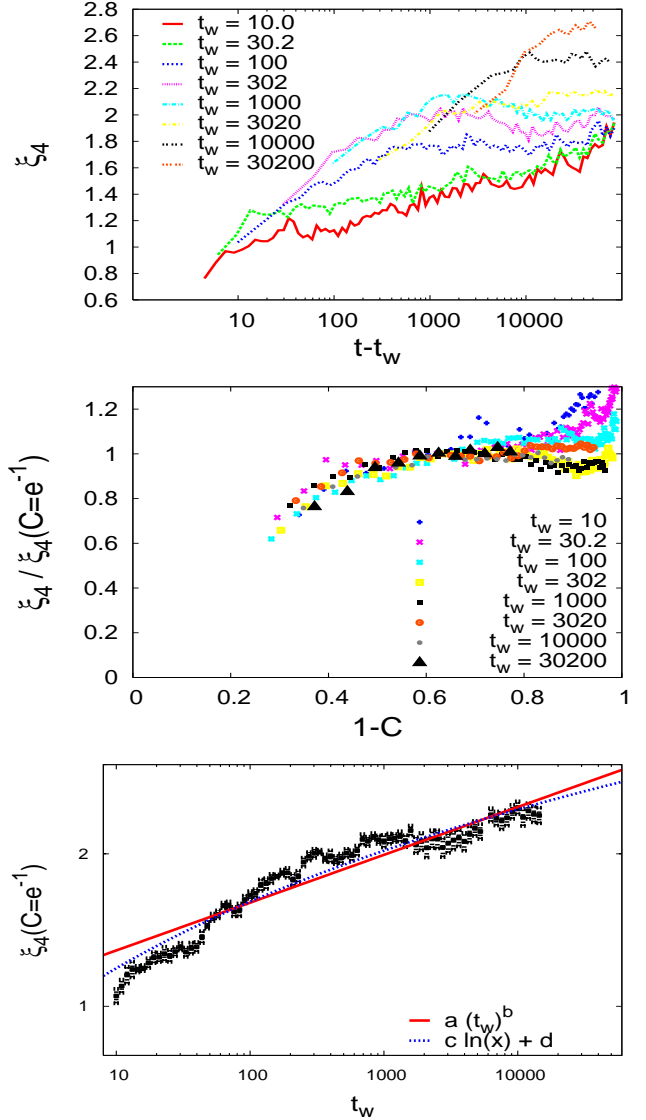


FIG. 2: (Color online) *Top panel*: Correlation length as a function of the time difference $t - t_w$. For small time differences ξ_4 is a function of $t - t_w$ only, but as $t - t_w$ increases, ξ_4 depends both on t_w and $t - t_w$. *Middle panel*: Rescaled ξ_4 versus $1 - C$. *Bottom panel*: Rescaling factor of the correlation length, $\xi_4(C = 1/e)$, versus the waiting time. The straight line is a fit to $\xi_4(C = 1/e) = a (t_w)^b$, with parameters $a = 1.037 \pm 0.027$ and $b = 0.094 \pm 0.003$. The other line is a logarithmic fit: $\xi_4(C = 1/e) = c \ln(x) + d$, with parameters $c = 0.182 \pm 0.005$ and $d = 0.768 \pm 0.033$.

which the peak occurs both grow as a function of t_w . As we anticipated above, we test for a possible scaling behavior with $C = C_{\text{global}}$ by plotting, in the middle panel of Fig. 1, the rescaled quantity $\chi_4 / \chi_4(C = 1/e)$ as a function of $1 - C$. We observe that all curves approximately collapse onto a single master curve. Thus

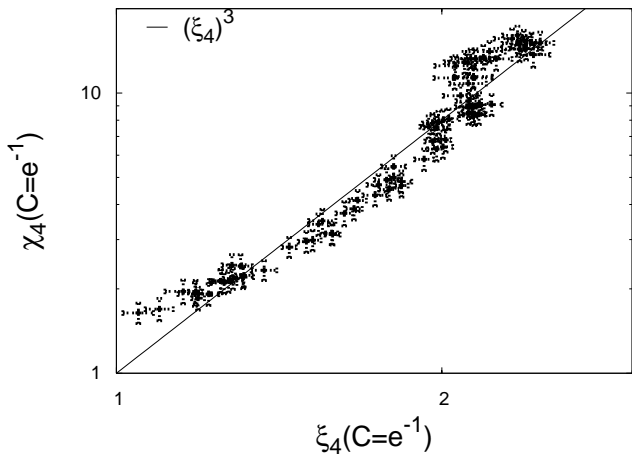


FIG. 3: Behavior of the 4-point density susceptibility rescaling factor versus the dynamic correlation length rescaling factor. The straight line corresponds to $\chi_4 = (\xi_4)^3$

we can say that $\chi_4(t, t_w) \approx \chi_4^\circ(t_w)\phi(C(t, t_w))$, where $\chi_4^\circ(t_w) \equiv \chi_4(t, t_w)|_{C(t, t_w)=1/e}$; a rescaling factor that depends only on t_w , and $\phi(C(t, t_w))$ is a scaling function which depends on times only through the value of the intermediate scattering function $C(t, t_w)$. As we see in the bottom panel of Fig. 1, the rescaling factor as a function of t_w can be fitted with the power law form $\chi_4^\circ(t_w) = at_w^b$, with the power $b = 0.277 \pm 0.008$.

We now extract a dynamic correlation length $\xi_4(t, t_w)$ from the 4-point correlation function $g_4(\mathbf{r}, t, t_w)$. By Fourier transforming the correlation function $g_4(\mathbf{r}, t, t_w)$ we obtain the 4-point dynamic structure factor $S_4(\mathbf{q}, t, t_w)$ and then fit the small q behavior with the form: $S_4(\mathbf{q}, t, t_w) = S_4(|\mathbf{q}| \rightarrow 0, t, t_w) \times \left\{ \frac{B}{1 + [|\mathbf{q}|\xi_4(t, t_w)]^\gamma} + (1 - B) \right\}$, where we find that the exponent $\gamma = 2.5$ gives the best fits.

The top panel of Fig. 2 shows the correlation length ξ_4 as a function of the time difference $t - t_w$ for $t_w = 10, \dots, 30200$. We see two regimes in this plot: i) the quasi-equilibrium regime ($t - t_w \lesssim t_w$), where ξ_4 is approximately time translation invariant (i.e. it depends on $t - t_w$ but *not* on t_w), and ii) the aging regime ($t - t_w \gtrsim t_w$), where ξ_4 generally grows for increasing t_w at fixed $t - t_w$. At fixed waiting time t_w , ξ_4 either grows or stays approximately constant as a function of $t - t_w$, but never decreases. Simulations in the supercooled regime show divergent results on this issue: in Ref.¹³ the correlation length increases initially, reaches a maximum and goes to zero for long time differences, while in Ref.¹⁴ the correlation length always grows with time difference. Similarly to χ_4 , the correlation length ξ_4 also displays an approximate scaling behavior with C_{global} : in the middle panel of Fig. 2, we plot $\xi_4/\xi_4(C = 1/e)$ as a function of $1 - C$. For not too small values of C all of the curves collapse onto a single master curve and

we can conclude that $\xi_4(t, t_w) \approx \xi_4^\circ(t_w)\phi(C(t, t_w))$ where $\xi_4^\circ(t_w) \equiv \xi_4(t, t_w)|_{C(t, t_w)=1/e}$, at least for $C \gtrsim 0.2$. At small $t_w \leq 30.2$, the values of ξ_4 keep growing as C decreases below 0.2, but for larger t_w the values of ξ_4 appear to stop growing and stay in a plateau. In the bottom panel of Fig. 2, we observe that the dependence of the scaling factor $\xi_4^\circ(t_w)$ on t_w can be fit by a power law form $\xi_4^\circ(t_w) = a(t_w)^b$ where $b = 0.094 \pm 0.003$; but it can also be fit with a logarithmic form $\xi_4^\circ(t_w) = c \ln(t_w) + d$. Both fits are roughly equally good, but the power law fit is preferred because it is consistent with the physically motivated scaling $\chi_4^\circ \sim (\xi_4^\circ)^3$ (see below).

To test whether the value of $\chi_4(t, t_w)$ is controlled by the correlation volume $(\xi_4(t, t_w))^3$, we plot in Fig. 3 the susceptibility scaling factor $\chi_4^\circ(t_w)$ as a function of the correlation length scaling factor $\xi_4^\circ(t_w)$, and find that the data are indeed well represented by the form $\chi_4^\circ \approx (\xi_4^\circ)^3$ (see also Ref.¹¹). However, looking at the data in more detail reveals an additional variation of $\chi_4(t, t_w)$ that cannot be due to the correlation volume: if we compare the two plots of $\chi_4(t, t_w)$ and $\xi_4(t, t_w)$ versus the global correlation $C(t, t_w)$ at constant t_w (the middle panels of Figs. 1 and 2), we find that as $C(t, t_w) \rightarrow 0$, $\chi_4(t, t_w)$ almost reaches zero, but $\xi_4(t, t_w)$ increases or stays constant. Clearly, the evolution of χ_4 at constant t_w is controlled not only by the correlation length but also by the amplitude of the correlations.

We now turn to a brief discussion of the anisotropic spatial structure of the correlations. We compute the connected correlation function of one-dimensional displacements of particles in the x direction, $C_x(\mathbf{R}, t, t_w) \equiv \langle \delta x(\mathbf{R}, t, t_w) \delta x(\mathbf{0}, t, t_w) \rangle_c$, where $\delta x(\mathbf{R}, t, t_w)$ represents the average displacement along the x direction from time t_w to time t of the particles that are present at time t_w in a small box centered at point \mathbf{R} . As we see in Fig. 4, the correlation is anisotropic: the contours of constant C_x extend much further in the x direction than in the perpendicular direction, for all values of C_x considered. This may be interpreted as a manifestation of cooperative “string-like” motion, similar to the one observed in the supercooled regime²³. To test whether the scaling with C_{global} holds also for the spatial structure of the correlations, we plot the contours of constant correlation $C_x = 0.008$ for various time pairs that correspond to $C_{\text{global}} = 0.1, 0.3, 0.5$. In the right panel of Fig. 4, we observe that if the global correlation $C_{\text{global}}(t, t_w)$ is kept fixed, the contours of constant $C_x = 0.008$ are approximately independent of t_w , and that the range of the displacement correlation increases as C_{global} decreases.

To summarize, we have studied the dynamic spatial correlations of density fluctuations and displacements in the aging regime of a simple binary Lennard-Jones mixture. We have found that: i) As a function of the time difference $t - t_w$, the density susceptibility $\chi_4(t, t_w)$ increases, reaches a maximum, and goes down towards zero eventually. As the waiting time t_w increases both the position and height of the peak grow. This behavior is reminiscent of the changes in the peak position and height as a

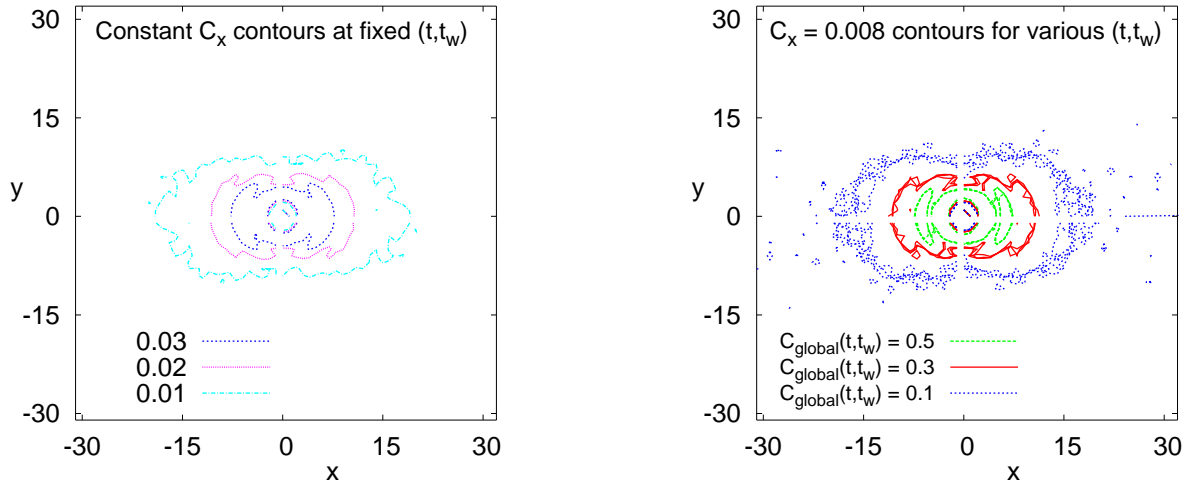


FIG. 4: (Color online) Correlation function $C_x(\mathbf{R}, t, t_w)$ of one-dimensional displacements along the x direction, plotted as a function of the x and y coordinates, for $\mathbf{R} = (x, y, 0)$. *Left panel:* Contours of constant correlation $C_x = 0.01, 0.02, 0.03$ for a single time pair: $t_w = 30.2, t = 2511.88$. The correlations extend more in the x direction than in the perpendicular direction. *Right panel:* Contours of constant correlation $C_x = 0.008$ for time pairs (t, t_w) that correspond to $C_{\text{global}}(t, t_w) = 0.1, 0.3, 0.5$. For each value of C_{global} , three time pairs (with $t_w = 100, 1000, 10000$) are plotted. As we see the contours of constant C_x are approximately independent of t_w at fixed C_{global} .

function of temperature in the supercooled regime^{12,13,14}.

ii) The dynamic correlation length $\xi_4(t, t_w)$ associated with density fluctuations increases both with the time difference $t - t_w$ and the waiting time t_w , and we *do not* observe any clear decrease for $t - t_w \gg t_w$. iii) Both the density susceptibility $\chi_4(t, t_w)$ and the correlation length $\xi_4(t, t_w)$ can be approximately factorized as products of a t_w -dependent scale times a scaling function that depends only on the value of the intermediate scattering function $C(t, t_w)$. In both cases, the t_w -dependent scale exhibits a power law growth as a function of t_w . iv) The values of the scales $\chi_4^\circ(t_w)$ and $\xi_4^\circ(t_w)$ approximately related by $\chi_4^\circ(t_w) \approx (\xi_4^\circ(t_w))^3$, consistent with the density susceptibility being proportional to the correlation volume. However the evolution of $\chi_4(t, t_w)$ and $\xi_4(t, t_w)$ at constant t_w is dissimilar: while $\chi_4(t, t_w) \rightarrow 0$ for large $t - t_w$, $\xi_4(t, t_w)$ does not appear to decrease for large $t - t_w$. This indicates that the integrated susceptibility $\chi_4(t, t_w)$ is not solely controlled by the behavior of the

correlation volume $(\xi_4(t, t_w))^3$, but also by the amplitude of the correlations. v) The spatial correlation function of displacements is anisotropic, with a longer range along the displacement direction than in the perpendicular direction, as a consequence of the cooperative nature of the motion. vi) The spatial correlation function of displacements scales with $C_{\text{global}}(t, t_w)$, i.e. it is approximately independent of t_w at fixed $C_{\text{global}}(t, t_w)$, and the range of this correlation function increases as C_{global} decreases.

H. E. C. especially thanks C. Chamon and L. Cugliandolo for very enlightening discussions over the years, and J. P. Bouchaud, S. Glotzer, N. Israeloff, M. Kennett, D. Reichman, and E. Weeks for suggestions and discussions. This work was supported in part by NSF under Grant PHY99-07949 and by Ohio University. Numerical simulations were carried out at the Ohio Supercomputing Center and at the Boston University SCV. H. E. C. acknowledges the hospitality of the Aspen Center for Physics.

¹ R. Zallen, *The physics of amorphous solids*, Wiley, New York, 1983.

² J.-P. Bouchaud, L. F. Cugliandolo, J. Kurchan, and M. Mézard, in *Spin glasses and random fields*, A. P. Young, ed., World Scientific, Singapore, 1998, cond-mat/9702070.

³ M. D. Ediger, *Annu. Rev. Phys. Chem.* **51**, 99 (2000).

⁴ H. Sillescu, *J. Non-Crystal. Solids* **243**, 81 (1999).

⁵ W. K. Kegel and A. V. Blaaderen, *Science* **287**, 290 (2000).

⁶ E. R. Weeks, J. C. Crocker, A. C. Levitt, A. Schofield, and

D. A. Weitz, *Science* **287**, 627 (2000); E. R. Weeks and D. A. Weitz, *Phys. Rev. Lett.* **89**, 095704 (2002), cond-mat/0107279.

⁷ R. E. Courtland and E. R. Weeks, *J Phys C* **15**, S359 (2003), cond-mat/0209148.

⁸ E. V. Russell, N. E. Israeloff, L. E. Walther, and H. Alvarez Gomariz, *Phys. Rev. Lett.* **81**, 1461 (1998), cond-mat/9807126; L. E. Walther, N. E. Israeloff, E. Vidal-Russell, and H. Alvarez Gomariz, *Phys. Rev. B* **57**, R15112

- (1998).
- ⁹ E. Vidal-Russell and N. E. Israeloff, *Nature*, **408**, 695 (2000), cond-mat/0012245.
- ¹⁰ K. S. Sinnathamby, H. Oukris, and N. E. Israeloff, *Phys. Rev. Lett.* **95**, 067205 (2005), cond-mat/0412378.
- ¹¹ G. Parisi, *J. Phys. Chem. B* **103** 4128-4131 (1999)
- ¹² W. Kob, C. Donati, S. J. Plimpton, P. H. Poole, and S. C. Glotzer, *Phys. Rev. Lett.* **79**, 2827 (1997), cond-mat/9706075; S. C. Glotzer, *J. Non-Crystal. Solids* **274**, 342 (2000).
- ¹³ N. Lacey, F. W. Starr, T. B. Schroder and S. C. Glotzer, *J. Chem. Phys.* **119**, 7372 (2003).
- ¹⁴ C. Toninelli, M. Wyart, L. Berthier, G. Biroli, J. P. Bouchaud, *Phys. Rev. E* **71**, 041505 (2005), cond-mat/0412158.
- ¹⁵ C. Chamon, M. P. Kennett, H. E. Castillo, and L. F. Cugliandolo, *Phys. Rev. Lett.* **89**, 217201 (2002), cond-mat/0109150.
- ¹⁶ H. E. Castillo, C. Chamon, L. F. Cugliandolo, and M. P. Kennett, *Phys. Rev. Lett.* **88**, 237201 (2002), cond-mat/0112272.
- ¹⁷ H. E. Castillo, C. Chamon, L. F. Cugliandolo, J. L. Iguain, and M. P. Kennett, *Phys. Rev. B* **68**, 134442 (2003), cond-mat/0211558.
- ¹⁸ C. Chamon, P. Charbonneau, L. F. Cugliandolo, D. R. Reichman, and M. Sellitto, *J. Chem. Phys.* **121**, 10120 (2004), cond-mat/0401326.
- ¹⁹ H. E. Castillo and A. Parsaeian, submitted (2006).
- ²⁰ C. Donati, S. C. Glotzer, and P. H. Poole, *Phys. Rev. Lett.* **82**, 5064 (1999), cond-mat/9811145.
- ²¹ W. Kob and J. L. Barrat, *Phys. Rev. Lett.* **78**, 4581-4584 (1997), cond-mat/9704006.
- ²² P. G. Debenedetti and F. H. Stillinger, *Nature* **410**, 259 (2001).
- ²³ C. Donati, J. F. Douglas, W. Kob, S. J. Plimpton, P. H. Poole, and S. C. Glotzer, *Phys. Rev. Lett.* **80**, 2338 (1998), cond-mat/9706277.